$\vec{k}\cdot\vec{p}$ perturbation theory in semiconductor alloys*

Eric D. Siggia†
Department of Physics, Harvard University, Cambridge, Massachusetts 02138
and Bell Laboratories, Murray Hill, New Jersey 07974
(Received 8 July 1974)

The conduction-band and valence-band edges in InSb-As, In-GaAs, and In-GaSb with spin-orbit splitting removed are calculated as a function of concentration. A two-band Kane model modified by a diagonal self-energy describing the intraband alloy scattering is used. Random strains decrease the band gap and increase the Kane formula mass. Experimental agreement is good. The spin-orbit splitting at Γ predicted for InSb-As disagrees with experiment. A proper treatment of alloy scattering does not appreciably alter the determination of the effective mass from transport measurements.

INTRODUCTION

There has been considerable theoretical interest in recent years in the electronic properties of binary alloys in which neither the concentration x, nor some measure of the random potential δ, are valid expansion parameters.[1-6] The problems of random systems, of which substitutional alloys represent the simplest example, have proved formidable enough that most papers deal with model Hamiltonians. The model calculations permit a test of competing approximations of which the so-called coherent-potential approximation (CPA) and generalizations to it have proved superior.[1,2] This paper applies a soluble model to a class of alloys which have been studied in detail experimentally.

The direct-gap III-V semiconductors GaAs, InAs, GaSb, and InSb with either a common cation or anion may be alloyed in arbitrary concentrations and show continuously variable properties intermediate between their parent components.[7] The alloys are substitutional and preserve the zinc-blende structure. Though size effects produce strains, there is no topological disorder.[8] Optical experiments show considerable structure, but most measurements have been of the direct gap, the spin-orbit splitting at Γ, and the conduction-band mass. Section I contains a brief discussion and references to these experiments along with some structural data. The effective mass, spin-orbit splitting, and band gaps are graphed to facilitate comparison with theory in Figs. 1–3.

The bulk of the experimental data could be explained by a theoretical treatment of the zone center. Kane has shown that $\vec{k}\cdot\vec{p}$ perturbation theory is the most economical way to describe a limited region of the Brillouin zone.[9] A modification of this theory with a cell-localized random potential is applied to semiconductor alloys. We feel it is probably the simplest possible theory within which to consider most of the effects of disorder in semiconductors. A coherent-potential calculation then gives a self-energy whose real part shifts the band edges and whose imaginary part represents the damping. Our model applies directly to the conduction band, but a complete description of the valence bands would involve the mixing of the three hole bands by the random potential. The simplicity of the CPA is lost once the self-energy is off-diagonal and momentum dependent. We argue that the displacement of the center of energy of the valence band is calculable within a one-band model and that the spin-orbit splitting may be computed separately as in pseudopotential band calculations.[10] The justification for such a theory, the evaluation of the parameters entering it, and its predictions for the effective mass, band gap, and spin-orbit splitting, are the subject of Sec. II and the principal result of this paper.

The optical properties of semiconductor alloys tend to be nearly as sharp as for crystals where it is a consequence of periodicity. Phillips argues that this qualitative feature of the data results from complicated coherent rearrangements of atomic positions that restore sharp band edges.[11-13] Our model does not contain these features, but is sufficiently simple that some approximate theories may be applied to the blurring of critical features. We discuss the necessity for self-consistent adjustments of atomic positions and the effects of random strains in the light of our theoretical estimates in Sec. II.

All experiments, to the best of the author's knowledge, have been done with the Fermi level in the bottom of the conduction band where a one-band model should adequately describe the alloy scattering. For lack of suitable theory, experiments have been analyzed as if the alloys were crystalline. If our theoretical description is to be consistent, one must go back and examine how a proper treatment of alloy scattering will affect the interpretation of experimental data. We derive

new transport expressions, where necessary, and evaluate them numerically, with parameters appropriate to the semiconductor alloys, in Sec. III.

In the conclusion we attempt to evaluate the errors inherent in our model and the discrepancies with experiment. We include also a brief discussion of some other theoretical work on semiconductor alloys.

I. EXPERIMENTAL BACKGROUND

The majority of the experiments on III-V alloys are due to J. C. Woolley and collaborators. The most extensive data exist for the alloy systems $In_{1-x}Ga_xSb$, $In_{1-x}Ga_xAs$, and $InSb_{1-x}As_x$. The latter shows the greatest deviations from virtual crystal behavior and is consequently the most interesting. We know of no work on the fourth alloy of this series, $GaSb_{1-x}As_x$, or any reason why it should be more difficult to prepare than $InSb_{1-x}As_x$. Less extensive data exists on phosphorous containing alloys, certain aluminum compounds, and Ge-Si.[14]

The structural properties and phase diagrams of the three alloy systems we study were investigated by Woolley.[15] Anneal times on the order of a month were required for the two resolvable diffraction peaks in the quenched mixture to merge into one.[16] The most difficult alloy to prepare was $InSb_{1-x}As_x$.[16, 17] Deviations from Vegard's law of about a percent were found and x-ray lines remained broad after long anneals. It is not certain that InSb and InAs are miscible in all proportions. Transport measurements are made in most instances on n-type samples prepared by the horizontal Bridgeman method. Annealing times are less, and there would seem to be more room for error than in the above study. In a later study, samples of $InSb_{1-x}As_x$ in the range $0.30 \leq x \leq 0.58$ could not be prepared.[18]

The direct gap E_g is measured by optical absorption and electrofluorescence at room temperature.[20, 21] In the one case in which the spectra themselves are given for $In_{1-x}Ga_xAs$, the adsorption α has an exponential tail which falls off as $\exp(-E/0.03\ \text{eV})$.[21] The Urbach tail in pure GaAs is steeper than in the alloy and is attributed to charged impurities.[22]

The uncertainty in E_g is given by a vertical error bar in Figs. 1(a), 1(d), and 1(g), which plot the variation with concentration of the band gap with the spin-orbit interaction removed $E_g + \frac{1}{3}\Delta_0$. The uncertainty is largest for $In_xGa_{1-x}As$ because we have data from two groups which differ by 0.1 eV for intermediate concentrations: roughly three times the scatter about a smooth curve found by either group for any of the three alloy systems.[20] Only Woolley's data are plotted in Fig. 1(g). Values of Δ_0 have been determined by only one group with an estimated error of 0.01 eV.[23] For $In_{1-x}Ga_xSb$ the spin-orbit splitting was not reported and we relied on an interpolation scheme to prepare Fig. 1(g).[23] The figure would be slightly different if a linear interpolation between the crystalline spin-orbit parameters was made.

The spin-orbit splitting along Λ, Δ, and at Γ have been measured by electroreflectance on several occasions.[24, 25] Specimens of $InSb_{1-x}As_x$ for $0.35 \leq x \leq 0.65$ initially gave poor spectra and were not used. There was some difficulty in connecting the data for large and small x for some of the

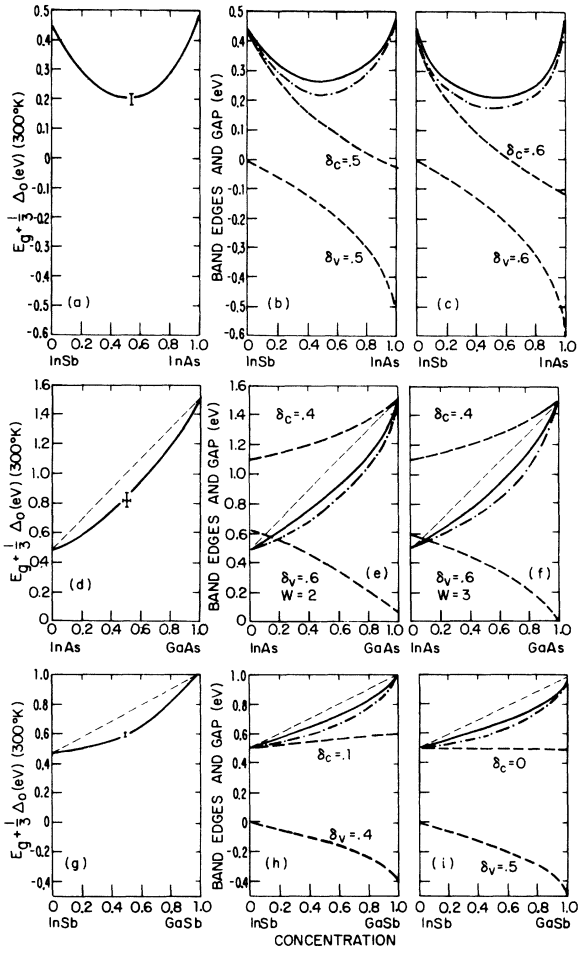

FIG. 1. (a), (d), and (g) represent measured band gaps with spin-orbit splitting removed. (b), (c), (e), (f), (h), and (i) represent theoretical predictions. The conduction bandwidths are 2.5 eV and the valence band-widths 2 eV except in (f), where it is 3 eV. Dashed line: the conduction and valence-band edges for the indicated impurity scattering potentials; solid line: difference of valence and conduction-band edges; dot-dash line: band gap corrected for random strains.

higher transitions and in interpreting the curvature of the data with varying concentration.[26] The lowest transitions and in particular Δ_0 (Fig. 2) seem to be free of these problems.

Transport measurements were made on n-type samples to determine the effective mass and, in some cases, Δ_0 and E_0.[17, 19, 26-31] The electron concentration n is determined by the Hall effect. Errors in n would affect the mobility or the effective mass as calculated from the plasma frequency or the Faraday angle. The high-field-saturation Hall coefficient and the plasma-edge reflectance were used for one determination of the effective mass.[26] A lifetime τ was extracted from the data which was of order $1/\omega_c$ for the highest magnetic fields used (32 kG). If the Boltzmann equation has any validity for alloys it is surprising that the Hall coefficient would saturate. By semiconductor standards, the transport measurements were made at a rather high concentration of donor (in some cases tellurium): up to 10^{19} cm^{-3} for the plasma reflectance. No impurity band was reported and experiments are all assumed to measure the conduction-band edge.[32] Extensive conductivity measurements are reported only for $InSb_{1-x}As_x$.[30]

The uncertainties in the effective mass are best judged by comparing the results for $InSb_{1-x}As_x$ by three different methods: plasma reflectance, Faraday rotation, and magneto-thermoelectric power [Fig. 3(a)].[26] The sample problems referred to above, the electronegativities of InSb and InAs, and the different lattice constants suggest that $InSb_{1-x}As_x$ should show the greatest deviations from linearity and the strongest alloy scattering. Most points fall within (10–15)% of the average curve, with the Faraday rotation showing the greatest deviations.

The room-temperature conduction-band effective masses and the Kane-formula prediction using the measured E_g and Δ_0 are plotted together in Figs. 3(a)–3(c).[33] The momentum matrix element appearing in the Kane formula is roughly constant for the III-V components we study.[34] The calculated mass lies several standard deviations below the measured value. The difference appears universally and is a problem for any theory of III-V alloys.

II. GENERALIZATION OF THE KANE MODEL TO ALLOYS

In this section we generalize the Kane model to alloys.[9] The theory provides a description of the center of the Brillouin zone and incorporates a qualitative treatment of the effects of random strains in addition to a coherent potential description of the random potential. A single propagator and self-energy characterize the states at the bottom of the conduction band, which simplifies the calculation of all the transport properties.

As the concentration tends to zero or one, the three alloys become six isovalent impurity-host systems, which serve as a guide in treating III-V

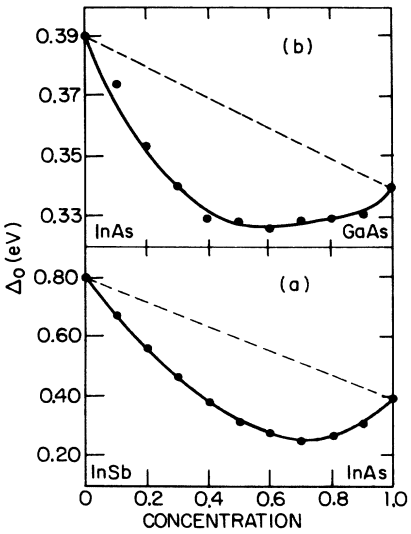

FIG. 2. Spin-orbit splitting at Γ.

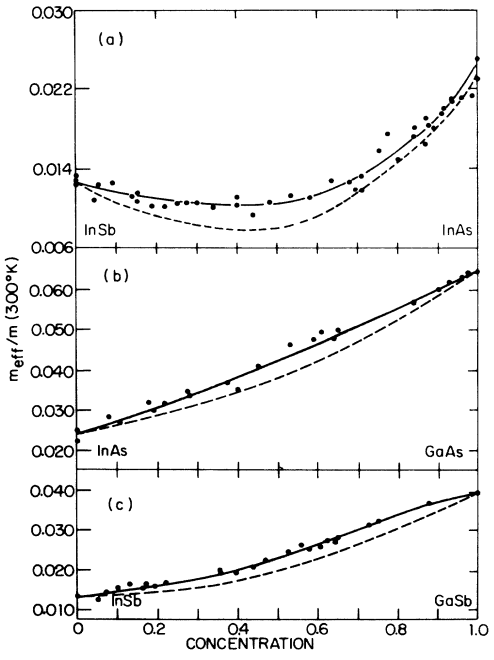

FIG. 3. Conduction-band effective masses. The solid line is the best fit to the data points. The dashed line is the calculated Kane formula mass found from the measured band gap and spin-orbit splitting as calculated in Ref. 41.

alloys.[35] Depending on the relative electronegativities of the substituent and host the impurity may trap either an electron or hole. The attraction is due to short-range forces since the impurities are uncharged, i.e., isovalent. Isovalent traps are generally miscible only in small proportions while GaAs:In, InAs:Sb, etc., do not bind a carrier and may be alloyed in all concentrations.

Baldereschi and Hopfield attempted to calculate which impurities would bind, and developed a detailed model of the impurity potential which we will carry over to the alloys.[36] They assumed a constant, wave-number-independent potential and used a Slater-Koster theory to compare it with the heavy-hole bandwidth. An electropositive impurity would pull a state out of the top of the valence band if the impurity potential were greater than the width of the narrowest band. The impurity is cell localized and its matrix elements between Bloch states are constants if one neglects the overlap of Wannier functions on neighboring sites—a reasonable first approximation. Baldereschi and Hopfield concentrated on evaluating the potential. Nearest-neighbor relaxation has an important effect on the local potential. When compared with experiment, Baldereschi and Hopfield explain the occurrence of traps correctly in seven out of eight cases. The agreement is not a very sensitive test of their model since most potentials are very small or quite large. If all potentials were scaled down by 30–40%, the agreement with experiment would be perfect.

Ionization energies are as much a surface as a bulk property.[37] The most optimistic assumption would be that the dipole-layer effects cancel in the difference and the uncertainty in the impurity potential is just twice the error found by comparing different measurements on clean surfaces, ± 0.3 eV.[38] The Baldereschi-Hopfield predictions are no more accurate than this. In Au-Ag alloys the relative work functions predict the direction of charge transfer incorrectly.[39]

For definiteness consider an alloy $AB_{1-x}B'_x$. The electrons feel a random array of potentials in a zinc-blende configuration with lattice constant $\bar{a}$ intermediate between a_{AB} and $a_{AB'}$. There will be some long-range lattice deformation, depending on the configuration of B and B' atoms. The ith atom is displaced by $\underline{\Delta}(\vec{R}_i)\cdot\vec{R}_i$. We define a random variable ϵ_i to be one if B' occupies an anion site $\vec{R}_i$, and zero otherwise. The average of ϵ_i is x. We compare the alloy to a pure AB crystal on a uniformly strained lattice of size $\bar{a}$. The difference between the two Hamiltonians, to lowest order, is the sum of two terms: a random strain field in a compositionally ordered material and a random impurity potential on a perfect lattice;

$$H_{ABB'}([\underline{1}+\underline{\Delta}(\vec{r})]\cdot\vec{r}) - H_{AB}(\vec{r}) = H_{AB}([\underline{1}+\underline{\Delta}(\vec{r})]\cdot\vec{r}) - H_{AB}(\vec{r}) + H_{ABB'}(\vec{r}) - H_{AB}(\vec{r}) \ . \tag{1}$$

In what follows we will make our decomposition of the Hamiltonian more precise, calculate the effects of strains in second-order perturbation theory, and apply the CPA to a model of random potentials on a perfect lattice. Our model is a generalization of the treatment of Baldereschi and Hopfield to arbitrary concentrations.

We define τ_i^α as the distance of the αth cation from its nearest-neighbor anion at R_i and $\bar{\tau}$ as the analogous quantity for a uniformly strained AB crystal. The second difference in Eq. (1), neglecting the correlation of strains among sites, is approximately

$$\frac{1}{4}\sum_{i,\alpha}(1-\epsilon_i)\{V_A[r-R_i-\tau_i^\alpha(B)]-V_A[r-R_i-\bar{\tau}]\} + \epsilon_i\{V_{B'}(r-R_i)+V_A[r-R_i-\tau_i^\alpha(B')] - V_B(r-R_i)-V_A(r-R_i-\bar{\tau})\} \ . \tag{2}$$

We sum over all anion sites and over the four nearest cation sites. The factor $\frac{1}{4}$ prevents double counting. The cations adjust their positions depending on which anions are nearest neighbors. In this manner the short-wavelength relaxation is included in the impurity potential while the long-wavelength components are contained in $\Delta(r)$. Such a division is more easily made on a lattice with several atoms per unit cell.

Although Eq. (2) contains a random variable and is not translationally invariant, we may construct a representation in terms of any complete set of functions. To generalize $\vec{k}\cdot\vec{p}$ perturbation theory for the zone center it is most natural to use the Kohn-Luttinger functions $e^{i\vec{k}\cdot\vec{r}}\chi_n(r)$ for an AB crystal with lattice constant $\bar{a}$.[40] The impurity potentials are short ranged and nonoverlapping. The wave-number dependence of a matrix element of $\sum_i \epsilon_i\,\delta V(r-R_i)$ factors as

$$\epsilon_{k-k'}\int\chi_n^*(r)\delta V(r)\chi_n(r), \quad \epsilon_{k-k'}=\sum_i e^{i(\vec{k}-\vec{k}')\cdot\vec{R}_i}\epsilon_i \ .$$

There is still T_d symmetry about the origin and the matrix element vanishes between bands of different symmetry. With a Bloch function basis and $k\neq 0$, an analogous statement could be made only if one neglected the overlap of Wannier functions on different sites. If all bands are retained the theory is exact and the random potential could, in principle, be treated as in the two-band model below. Within the 8×8 subspace spanned by the states at the gap, the inverse propagator has the same symmetry as in a crystal but the energies at Γ are

shifted by some self-energy dependent on concentration. A spin-orbit splitting Δ_0 and a gap E_g exist, and a Kane formula for the effective mass for a substitutional alloy follows just as for a crystal.[9] We have neglected the random strain field. The momentum matrix element is essentially the same (to within 2%) for all pairs of compounds alloyed.[34] The Kane mass calculated from the measured spin-orbit splitting and gap appears in Fig. 3.[41]

Several authors have noted the disagreement between the Kane-formula predictions and the effective mass.[19,41] We account for it semiquantitatively by calculating the effects of the strain term in Eq. (1). Firstly, there is a renormalization of the band gap parameters. Since we have used measured gaps, this effect is already included. The deformation potential arising from the long-range strain does not have T_d symmetry about the origin and thus couples $e^{i\vec{k}\cdot\vec{r}}\chi_v$ and $e^{i\vec{k}\cdot\vec{r}}\chi_c$. In second-order perturbation theory the momentum matrix element is reduced by a factor $1-D^2\langle\Delta\Delta\rangle/E_g^2$, where

$$\langle\Delta\Delta\rangle=\int\langle\Delta(k)\,\Delta(-k)\rangle\,d^3k$$

is the mean-square dilation coupling the valence and conduction bands. Only k-dependent strain fields break the tetrahedral symmetry. If we take the cross deformation potential D as 3 eV/dilation, the smaller of the absolute valence-band and conduction-band deformation potentials,[42] we estimate the correction to p as

$$1-3^2x(1-x)\left[3(a_1-a_2)/\bar{a}\right]^2 .$$

The average gap is roughly 1 eV. Including piezoelectric effects in addition to the deformation potential does not appreciably modify this estimate.[11] The maximum correction to the Kane-formula mass is a twenty percent increase at $x=\frac{1}{2}$. This agrees within experimental error (Fig. 3), but is nothing more than a crude estimate.

We argue, for our purposes, that the band gap with spin-orbit splitting removed may be calculated within a two-band Kane model. For a single impurity it was sufficient to include only the narrowest valence band to determine whether a bound state occurred. On the alloy we assume the valence-band center of energy is due to the interactions of the point Γ with a band 2–3 eV wide: the distance from the band edge to the dip in the density of states at the lower edge of the heavy hole band. A much more complicated three-band model would be needed to calculate the separate valence band masses and damping near Γ. In what follows, the effects of the random potential on the band bap and transport will be calculated with the Hamiltonian

$$H=\begin{pmatrix}\frac{k^2}{2m}+E_v^0 & \frac{-ik_ip}{m}\\ \frac{ik_ip}{m} & \frac{k^2}{2m}+E_c^0\end{pmatrix}\delta(k-k')+\begin{pmatrix}\delta_v & 0\\ 0 & \delta_c\end{pmatrix}\epsilon_{k-k'}, \tag{3}$$

where ϵ_q is the Fourier transform of the random variable ϵ_i, the $\delta_{v,c}$ are the valence- and conduction-band potentials, and the $E_{v,c}^0$ are the valence- and conduction-band energies at $k=0$ of an AB crystal.

The impurity potentials $\delta_{v,c}$ are matrix elements of Eq. (2) between Kohn-Luttinger states and may be estimated by the methods proposed by Baldereschi and Hopfield.[36] The arithmetic is more tedious since we imagine substituting with probability x and $1-x$, respectively, both AB and AB' unit cells into a host which is a uniformly strained AB crystal. Measured relative to the *unstrained* AB crystal, the coefficient of the random variable ϵ_i is roughly the difference in ionization potentials. Efforts to refine this estimate are not worth while since, as a measure of bulk properties, the ionization potential is not accurate to more than 0.1–0.2 eV.[38] The valence- and conduction-band potentials are both uncertain by ±0.3 eV, but their difference must be the band gap which is known to 0.05 eV. Table I lists the ionization potential averaged over the heavy-hole band and the band gap with spin-orbit splitting removed.[10,43] The differences are the valence- and conduction-band impurity potentials.

In order to calculate a self-energy from the random potential with the coherent-potential approximation, we need the free-particle density of states $\rho(E)$. Equation (3) is valid only for small wave numbers, so we replace all momentum sums by an integral over $\rho(E)$. For numerical simplicity, and since we are only interested in states near the band edge, we use a semicircular density[2] whose width corresponds to the cutoff, 2–3 eV for the valence band and 2.5 eV for the conduction band. The latter number is just the width of the lowest conduction band.[10] The result of all our approximations is an effective Hamiltonian or

TABLE I. Averaged ionization potentials and band gaps.

	GaAs	GaSb	InAs	InSb
$\bar{I}$ (eV)	7.0	6.1	6.4	5.7
$\bar{I}-E_g-\frac{1}{3}\Delta_0$ (eV)	5.5	5.1	5.9	5.2

inverse propagator:

$$E - G^{-1} = \begin{pmatrix} E_c^0 + \Sigma_c(E) + \frac{k^2}{2m} & \frac{-ik_i p}{m} \\ \frac{ik_i p}{m} & E_v^0 + \Sigma_v(E) + \frac{k^2}{2m} \end{pmatrix} . \tag{4}$$

The real parts of $\Sigma_{v,c}$ shift the band edge from $E_{v,c}^0$ to $E_{v,c}$ and the imaginary parts are only nonzero below (above) $E_{v,c}$. In the low concentration limit $\Sigma(E) = x\delta/[1 - \delta G(E)]$, which has a pole where the Slater-Koster theory predicts a bound state. In this sense our approximations amount to a generalization of the Baldereschi-Hopfield Theory to finite concentrations. Within a mean-field theory the band edges still vary as $\sqrt{E}$. Near the conduction-band edge

$$G = \left[E - E_c - \Sigma_c(E) - \frac{k^2}{2m_{\text{eff}}}\right]^{-1} ,$$
$$\frac{1}{m_{\text{eff}}} = \frac{1}{m} + \frac{2p^2}{m^2(E_c - E_v)} . \tag{5}$$

If Fig. 1 we have plotted the valence and conduction band edges $E_{v,c}$ due to the random potentials. The curvature of $E_{v,c}$ may be understood by ordinary perturbation theory. The density of states for a given band is limited to the union of the host band with the host band shifted by δ. When a finite concentration of positive impurity is added, the top of the band moves upward more rapidly than the bottom. When $x = 1$, the entire band just translates by δ, but for intermediate x it is wider than in the crystal. In an extreme case, when δ is much greater than the band width, an impurity band splits off and the upper (lower) band edges jump by δ at $x = 0$, (1). Narrower bands or larger impurity potentials increase the nonlinearity.

There are two theoretical plots in Figs. 1(b)–1(i) to show how variations in potentials or band widths affect the band gap. The valence band widths are all 2 eV, expect in Fig. 1(f), and all conduction bands are 2.5 eV wide. Table II gives the fitted potentials which agree to within a few tenths of a volt to the differences of the absolute potentials in Table I. We have fit our curves to the measured room-temperature gaps. At zero temperature Figs. 1(a), 1(d), and 1(g) would be 0.05–0.1 eV higher, and δ_c would be shifted by a corresponding amount to give the correct gaps at $x = 0$, 1.[44] The predicted zero-temperature band gap could be lowered by 0.05–0.1 eV for comparison with the data at 300 °K. A fit of the potentials to the room temperature gaps is in error by no more than the difference in temperature shifts (≤ 0.05 eV), and the predicted room temperature gap is even less in error. The temperature coefficient of Δ_0 is an order of magnitude less than the coefficient of E_0.[45] The difference of E_c and E_v appears as a heavy line in Fig. 1. It does not seem possible to measure $E_{c,v}$ separately to 0.1 eV accuracy.

The random-strain field is a further correction to the band gap calculated from the random potentials. The off-diagonal corrections to G^{-1}, Eq. (4), were estimated by second-order perturbation theory. For the diagonal terms or the band gap, the renormalization may be computed more accurately by simply rescaling the pseudopotential form factors by the Debye-Waller factor $\exp(-\frac{1}{6}G^2\langle u^2\rangle)$.[11,46] The phonon frequency does not enter the Debye-Waller factor; so the effects of strains may be calculated using for $\langle u^2\rangle$ the mean-square strain at a site. In simple pseudopotential models the energy gap scales as the sum of $V(220)$ and $V^2(111)$.[11] For our purposes the Debye-Waller factors are the same and we scale the theoretical gaps by $\exp[-(2\pi)^2\langle u^2\rangle]$. An upper estimate for $\langle u^2\rangle$ is given in terms of the mismatch of lattice constants and the concentration, $3x(1-x)[(a_1-a_2)/a]^2$. The scale factors are $\exp[-0.6x(1-x)]$, $\exp[-0.5x \times (1-x)]$, and $\exp[-0.4x(1-x)]$ for $InSb_{1-x}As_x$, $In_{1-x}Ga_xAs$, and $In_{1-x}Ga_xSb$, respectively. The band gap with strain is shown by a dashed-dotted line in Fig. 1. Our estimates are rather crude and could be improved if the Debye-Waller factors were known from x-ray measurements. The strain corrections are fortunately small and the overall agreement of the band gap with experiment is good.

The spin-orbit splitting comes primarily from the core regions and cannot be calculated from pseudopotentials. In first-order perturbation theory

$$\Delta_0 = -3i(\hbar/4m^2c^2)\langle\psi_x|(\vec{\nabla}V\times\vec{p}_y|\psi_z\rangle , \tag{6}$$

where V is the actual atomic-core potential and the wave functions are either tight binding or a pseudo wave function at Γ, weighting an atomic p function.[9,47] The atomic functions in ψ are cell localized, so their relative phases, the same for all p states, do not enter Δ_0.

For an alloy, we argue that a configuration average of Eq. (6) may again be used where the wave functions and core potentials are random. In a given configuration, the wave function at Γ of the alloy $AB_{1-x}B'_x$ has an amplitude on the anion sites

TABLE II. Impurity potentials fitted to experiment.

	InAs : Sb	In : GaAs	In : GaSb
Valence band δ_v (eV)	0.5	0.6	0.4
Conduction band δ_c (eV)	0.5	−0.4	−0.1

depending on whether B or B' is present. The phase is irrelevant for our purposes. The amplitude on the cation sites, occupied by A, depends in some complicated way on the occupancy of the nearest-neighbor anion sites. This correlation effect cannot be treated within mean-field theory and, furthermore, is small. The cation amplitudes fluctuate between their values in AB and AB', which are only a few percent different.[48]

On the anion sites we construct a wave function whose amplitude at R_i is the one-band tight-binding wave function ϕ_i multiplied by the atomic p function appropriate to the site: $\epsilon_i\psi_{B'}(r-R_i)+ +(1-\epsilon_i)\psi_B(r-R_i)$. For the core potential we use an atomic potential B, B', according to the occupancy of the anion sites. Averaging over configurations and converting to second-quantitized form, Eq. (6) becomes

$$\Delta^{AB_xB'_{1-x}} = \Delta^{AB} + (\Delta^{AB'} - \Delta^{AB}) \times \frac{\mathrm{Im}\langle\epsilon_1\phi_1^\dagger\phi_1\rangle(E)}{\mathrm{Im}\langle\phi_1^\dagger\phi_1\rangle(E)}\bigg|_{E=E_v} . \tag{7}$$

By assumption, the spin-orbit splitting at A may be simply added on to the contribution from anion sites to give the complete alloy or crystalline splitting. The numerator expresses the correlation between the occupancy of a site and the amplitude of the wave function. The imaginary part gives the spectral function. We have divided by the density of states since we want the matrix element of Eq. (6) for one state, not per unit of energy.

In the CPA,

$$\langle\epsilon_1\phi_1^\dagger\phi_1\rangle(E) = G(E)\,\Sigma(E)/\delta ,$$

which may be evaluated numerically near the band edge. For our purposes, we keep just the two lowest terms in Σ in order to rewrite Eq. (7) as

$$\Delta(x) = \Delta^{AB} + (\Delta^{AB'} - \Delta^{AB})\left[x + x(1-x)\,2\delta\,\mathrm{Re}G(E_v)\right]. \tag{8}$$

The quantity δ is the potential of AB' in an AB host. From numerical calculations, $\mathrm{Re}G(E)$ varies from 1.5 to 2 as x varies from 0 to 1, δ from 0 to $\frac{1}{2}$, and the energy from the band edge to -0.20 eV. The CPA is inexact near the band edge and we estimate the corrections to the density of states below. Virtually nothing is known quantitatively about the wave functions near the band edge. The CPA is valid 0.20 eV below E_v and the rough consistency of $\mathrm{Re}G(E)$ over this energy range makes our approximation seem less dubious.

For all the alloys we consider, $\delta>0$ when $\Delta^{AB'} - \Delta^{AB} > 0$. Equation (7) or (8) implies that $\Delta^{AB_{1-x}B'_x}$ is a convex function of x. The physical reason for the sign of the curvature is similar to the explanation of the curvature of $E_{v,c}(x)$ and holds more generally than our numerical approximations. When a positively charged impurity is added to a band the states at the bottom of the band are concentrated on the host atoms, while by the exclusion principle the wave functions at the top of the band are more concentrated on impurity atoms. In the extreme case of $\delta \gg 1$ the top of the valence band would be an impurity band formed by AB'. In this case,

$$\Delta^{AB_{1-x}B'_x} = \Delta^{AB'} \text{ for } x>0 .$$

These trends are confirmed by model calculations of the spectral functions.[2] In $InSb_{1-x}As_x$, the wave functions at the top of the valence band spend more time in InSb than in InAs, hence the negative curvature.

We feel the positive curvatures shown in Fig. 2 contradict our theory only for $InSb_{1-x}As_x$. We have neglected the effects of strains which explained the disagreement between the effective mass and the Kane prediction. The second-order perturbation calculation we performed is equivalent to the assumption that in the presence of strains the valence and conduction bands contain states of s and p symmetry,

$$\psi_v^i = (1-\alpha^2)^{1/2}p_i + \alpha s$$

and

$$\psi_c = (1-\beta^2)^{1/2}s + \beta/\sqrt{3}\sum_1^3 p_i .$$

The momentum matrix element is reduced by

$$(1-\alpha^2)^{1/2}(1-\beta^2)^{1/2} + \alpha\beta/\sqrt{3} < (1-\alpha^2)^{1/2}(1-\beta^2)^{1/2}$$

and the Kane mass increased by its reciprocal squared. The spin-orbit splitting is reduced by $1-\alpha^2$. This scale factor is applied to $\Delta(x)$ while Eq. (7) corrects the virtual crystal theory by a term of order $\Delta^{AB'} - \Delta^{AB}$. For $In_{1-x}Ga_xAs$, a small concentration-dependent admixture of s-wave symmetry into ψ_v would account for the observed curvature in Δ and the correction to the Kane-formula mass. To explain the $InSb_{1-x}As_x$ data, however, $1-\alpha^2 \sim \frac{1}{2}$, which would mean at least doubling the Kane predictions for the effective mass which are then in disagreement with experiment in Fig. 3. For $ZnTe_{1-x}Se_x$ our theory works relatively well, as we discuss in the conclusion.

At the band edge, the CPA predicts the experimental behavior

$$\rho(E) \sim |E - E_{v,c}|^{1/2}$$

which, however, is not rigorously correct for our model Hamiltonian. Systematic calculations become difficult beyond the CPA and we resort to some less controlled approximations to estimate

our error at the band edge. Halperin and Lax developed a variational method for bounding the band tail caused by screened Coulomb impurities in semiconductors.[49] Their *Ansatz* is only tractable for a high density of weak scatters. An electron on any given site must feel the potential of many impurities. The tailing is measured relative to the virtual crystal edge, $E_c^0 - x\delta$ in our notation. In particular, their theory is invalid when a split-off impurity band exists and the density of states is no longer just a broadened band edge. We adapt their *Ansatz* to our tight-binding model in Appendix A. The approximation is only useful for $\delta < 0.3$, e.g., for the conduction bands of $In_{1-x}Ga_xAs$ and $In_{1-x}Ga_xSb$. The crude variational bound in Appendix A becomes

$$\rho(E) \sim \exp - |E - x\delta/\Delta|^{1/2} ,$$

$$\Delta = (xy\delta^2)^2 (25 m_{\text{eff}}/m)^3 \, 10^{-5} \text{ eV} .$$

For small δ the tailing is completely negligible, which is not surprising, since the band edge varies according to the virtual-crystal theory.

Anderson has calculated the localization of a charge by a random-cell potential.[50] Anderson's model applies better to a III-V alloy than to amorphous germanium where it is often used.[51] For the model, there exist semiquantitative estimates of the mobility edge—the energy at which states become localized.[51] Since the CPA conductivity is nonzero whenever the density of states is finite, the mobility edge should be at or near the band edge. For a band of width 2 and edges at ± 1, the mobility edge formed when a concentration x of impurity potential δ is added satisfies

$$-x \ln|E - \delta| = (1 - x) \ln|E| .$$

The equation is unchanged if the host and impurity are reversed

$$x \to 1 - x, \quad E \to -E + \delta .$$

The approximations are similar to those in Anderson's original paper.[50] Figure 4 is a graph of the mobility and band edges. The level of our quantitative understanding of the Anderson model precludes attaching any significance to the mobility gaps in Fig. 4 other than that they are small. We do not find published explanations of the relatively sharp optical edges in semiconductor alloys compelling.[11-13]

III. TRANSPORT PROPERTIES

We have compared theory with experiments analyzed as if the materials were crystalline. All experiments were run on n-type samples with E_f generally within a few tenths of a volt of the band edge. The CPA and Eq. (5) (with the measured effective mass) should be good approximations except for the neglect of nonparabolic effects. Our numerical results cannot be considered more than semiquantitative. We reexamined only those experiments in which alloy scattering is expected to be important and the electron gas is degenerate. The thermoelectric power at room temperature is dominated by phonon scattering and was not considered.[27] The conductivity lifetime is also dominated by phonons at room temperature but we calculated it to compare with the measured values and to illustrate what a low temperature measurement on clean samples should give. For the plasma edge reflectance and Faraday rotation, we calculate small deviations from free-particle behavior which are probably within experimental uncertainty. Within the CPA, vertex corrections to most transport coefficients vanish. Calculations are simple and have been performed by a number of authors.[3,4] In a few cases it has been necessary to derive new expressions, but the purpose of this section is to give numerical results for the three alloys we consider.

We define α and β to be the real and positive imaginary parts of $(E - E_c^0 - \Sigma_c(E))^{1/2}$ and understand that when the argument E is not written they are evaluated at the Fermi surface. The zero-magnetic-field conductivity defines a lifetime

$$\frac{m\sigma}{ne^2\hbar} \equiv \frac{\tau}{\hbar} = \alpha^2 \Big/ \left(6\beta \int_{-\infty}^{E_F} \alpha(E)\, dE \right) \sim \frac{1}{2\Sigma_c''(E_F)} .$$

We list a few values in Table III. Our calculated lifetime is somewhat shorter than that measured in $InSb_{1-x}As_x$ at room temperature where the mobility is dominated by polar scattering.[31,32,52] The CPA doesn't apply to states in the band tail and in these experiments $E_F \leq 300\,^\circ$K. There is some discrepancy to a lifetime fit to reflectance data.[26]

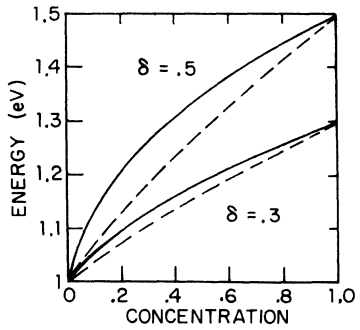

FIG. 4. CPA prediction for the band edge (solid line) compared with the estimated mobility edge (dashed line) for two values of the impurity potential. The bandwidth is 2 eV.

The Hall coefficient R is defined as $\lim_{H\to 0}\sigma_{xy}/H\sigma_{xx}^2$. Its deviation from the free electron value is measured by

$$\gamma_0 \equiv necR = \frac{3}{2}\left(\int_0^{E_F}\alpha(E)\,dE\right)\Big/\,\alpha(\alpha^2+\beta^2)\ .$$

The conductivities depend only on Fermi-surface properties within the CPA, while the density requires an integration over all occupied states. The high-field Hall constant is difficult to calculate because the free particle density of states can no longer be assumed semicircular and is not expected to saturate at the fields used (see Sec. I). There is some evidence that for small E_F, γ_∞ is less than one in regions where γ_0 is greater than one.[4] Table IV lists some typical values. Except for large δ and $x=0.9$, $\gamma=1$ to a few percent, which is all the accuracy one can claim for the CPA.

The plasma frequency has been measured by reflectance.[26] In Appendix B we calculate $\epsilon(\omega)$ in the CPA. For the range of parameters used in the experiments and neglecting dampening, $\epsilon(\omega)$ is approximately

$$\epsilon_\infty - \frac{4\pi ne^2}{\omega^2\epsilon_0 m_{\rm eff}[1-\partial\Sigma'(E_F)/\partial E_F]^2}\ .$$

Table V lists some values of $1-\partial\Sigma'/\partial E$. It depends only weakly on the energy. If the sample data were analyzed as for crystalline materials,

$$m_{\rm plasma} = m_{\rm eff}\,(1-\partial\Sigma'/\partial E)^2/\gamma\ .$$

The corrections are a maximum of 15% on the Sb-rich side of $InSb_{1-x}As_x$ which is still within experimental error. The corrections depended primarily on δ scaled by the bandwidth, which in Table V is two. The conduction band in $InSb_{1-x}As_x$ is normally 2.5 eV wide and $\delta\sim 0.5$ so a correction factor between $\delta=0.3$ and 0.5 has been used. The corrections are smaller for $In_{1-x}Ga_xAs$ and $In_{1-x}Ga_xSb$.

When Faraday rotation is calculated in the presence of alloy scattering, we find

$$m_{\rm faraday} = m_{\rm eff}\left(\frac{1-\partial\Sigma'/\partial E}{\gamma}\right)^{1/2}\ .$$

The correction factor is less than $m_{\rm plasma}/m_{\rm eff}$ and the experimental scatter is greater.

The most careful mass measurements reported are cyclotron resonance experiments at 4 °K on lightly doped samples.[19] In the quantum limit, the CPA calculated with just two Landau levels would determine the cyclotron frequency. (For the high-field Hall measurements, ten to twenty Landau levels are occupied.[26]) Unfortunately the application of the CPA so near the band edge is suspect.

CONCLUSION

We were motivated by the success of models of isovalent impurities to modify $\vec{k}\cdot\vec{p}$ perturbation theory with a band-diagonal k-independent self-energy. Near the band edge the self-energy should only depend on the magnitude of a local random-site potential scaled by the bandwidth. A tight-binding model which contained these two parameters was used in the numerical calculations. The self-energy shifts the band edge and predicts a finite lifetime for carriers. We argued that the effects of alloying on the valence-band center of energy and the spin-orbit splitting are accounted for by a one-band calculation. A two-band Kane model has the fewest parameters either to be fit to experiment or estimated from theory and has proven to satisfactorily explain the variable band gap.

At some points our derivation has been heuristic and we can only roughly estimate the errors committed. We have treated the strain field as random, independent of the alloy configuration, except for the relaxation of the nearest neighbors around an impurity. There, the displacement-induced potential is incorporated into the impurity potential. Correlations of displacements due to the proximity of several impurities are ignored. Such effects may have been observed in pair recombination spectra.[53] The long-range dilation has a negligible effect on the binding energy of a trap.[54] The magnitude may be estimated variationally knowing $\Delta(r)$, which falls off as $1/r^3$ and has zero angular average in a cubic material.[55]

Our theory applies only to direct gap materials in which the energy extrema remain at the same point in k space. We could not calculate the indirect gap as it moved along some symmetry direction with alloying. In a Kohn-Luttinger basis, bands of different symmetry do not couple through the random potential. The intraband effects are found more important than the interband couplings

TABLE III. Correction to hall coefficient $\gamma_0 = necR$.

Concentration		0.1	0.3	0.5	0.7	0.9
$\delta=0.3$	$E_F=0.1$	1.00	1.00	1.00	1.00	1.06
$\delta=0.5$	$E_F=0.1$	1.00	1.00	1.00	1.01	1.10

TABLE IV. Conductivity lifetime τ $(\text{eV})^{-1}$ $(\tau\propto 1/\sqrt{E_F})$.

Concentration		0.1	0.3	0.5	0.7	0.9
$\delta=0.3$	$E_F=0.1$	140	50	28	22	28
$\delta=0.5$	$E_F=0.1$	80	25	14	9	7

at Γ. The former are treated by the CPA, the latter in second-order perturbation theory or by a Debye-Waller factor. At an arbitrary point in the Brillouin zone this separation may not hold and our analysis would be complicated by an off-diagonal k-dependent potential and self-energy. At Γ, the most important interband mixing occurs through the strain field between the valence and conduction bands. Estimates of the corrections to the effective mass and spin-orbit splitting are easier to make than elsewhere in the zone. When working about a different point in the Brillouin zone, we would not expect the impurity potentials to be exactly the same as at Γ. Within the ±0.2–0.3 eV accuracy of the theoretical estimates the potentials are fit to experiments at a given symmetry point.

The spin-orbit splitting at Γ has been measured as a function of concentration for six alloy systems.[25] An impurity potential calculation corrects the linear approximation by a convex function proportional to $|\Delta_0^1 - \Delta_0^2|$. For all systems, except $InSb_{1-x}As_x$, the estimated admixture of s-symmetry states into the valence band would restore the observed curvature.[41] In $InSb_{1-x}As_x$ the magnitude of the disagreement of the Kane formula with the measured effective masses is much too small to account for observed curvature of Δ_0. If the wave function had greatly different amplitudes on the anions in the parent compounds, positive curvature could result.[48] A more important effect we have neglected is the mixing of valence states of different orbital symmetry into Γ by the random potential. Such effects would be contained in a four-band Kane model and would lead to a positive curvature. An experimental error seems unlikely.

Within our theory, Δ_0 is not a "band gap" between Γ_7 and Γ_8. The valence band cutoff extends beyond Δ_0 into the "split-off band" and it's not apparent whether Γ_7 is at the top or in the middle of a "band" when there is strong alloy scattering. First-order perturbation theory seems unambiguous.

There have been several theoretical attempts to deal with semiconductor alloys. The most complete was a study of Ge-Si by Stroud and Ehrenreich.[5] They exploited the constant difference of the pseudopotential form factors, $V(G)$, of Si and Ge, to use a separable random potential. A shifted and broadened band structure is computed within the CPA. The calculated dampening at Γ_2 was much too large, since this point differs in energy by a few volts in Si and Ge. The impurity potential in the III-V alloys is not separable. Numerical t-matrix calculations have met with some success in metallic alloys.[6] The full band structure with dampening was calculated, but the charge-transfer effects were an important determinant of the potential and best fit from experiments. Charge transfer is not as important in semiconductors, and is implicitly contained in $\delta_{v,c}$ when fit to experiment.

Richardson claims good agreement with experiment using a virtual-crystal model in which

$$V(G) = x\frac{a_1^3}{[xa_1 + (1-x)a_2]^3}\,V_1(G) + (1-x)\frac{a_2^3}{[xa_1 + (1-x)a_2]^3}\,V_2(G)\,,$$

where $a_{1,2}$ are the lattice constants and $V_{1,2}$ the pseudopotential form factors of the parent components.[56,57] The crystalline form factors are corrected for the change in lattice constant. Since the momentum-dependent pseudopotential is averaged, the band gap is not expected to vary linearly with concentration. Some additional curvature is introduced in the averaging, (e.g., through the average unit cell volume), whose importance can be estimated from the derivatives $dE_{\Gamma_{15}-\Gamma_2}/dV(G)$.[10] The quadratic term $6x(1-x)[(a_1-a_2)/(a_1+a_2)](V_1-V_2)(G)$ or lattice corrections to the form factors influence the direct gap by no more than 0.05 eV. It is not clear how the spin-orbit splitting is calculated. Richardson uses, for comparison, measurements of E_0 not $E_0 + \frac{1}{3}\Delta_0$. Richardson and Hill have measured and calculated the band gap of $ZnTe_{1-x}S_x$ for all concentrations.[57] The agreement is good, but both theory and experiment predict an isovalent trap in ZnS:Te which cannot be found by a virtual-crystal model.[36] It is somewhat surprising that these materials may be alloyed in all proportions.

Van Vechten *et al.* have explained both the corrections to the Kane-formula mass and the curvature of the spin-orbit splitting as valence-conduction mixing.[23,41] We find their method for calculating these corrections to be empirical.

Sen has recently applied the CPA to a two-band tight-binding model.[58] In his Hamiltonian the hopping term is diagonal in the band indices while the random term mixes the bands. His results would be qualitatively unchanged if the random term were diagonal and the overlap mixed the

TABLE V. Correction factors $1 - \partial\Sigma'(E_F)/\partial E_F$ (Sec. III).

Concentration		0.1	0.3	0.5	0.7	0.9
$\delta = 0.3$	$E_F = 0.1$	0.998	0.99	0.98	0.95	0.94
$\delta = 0.5$	$E_F = 0.1$	0.9994	0.993	0.98	0.94	0.80

bands as we have assumed for small k. It would be interesting to see whether a complete solution within the CPA of such a model would reproduce our results for the effective mass and the band gap.

After this paper was written, data appeared on the spin-orbit splitting at Γ in the ZnSe-Te system.[59] As a function of concentration, Δ_0 is convex and in approximate agreement with Eq. (7) evaluated within the CPA. Interband effects are smaller than in InSb-As because of the larger band gap, and our approximations should be better.

ACKNOWLEDGMENTS

This work was begun during the summer at Bell Laboratories. The author is grateful for the hospitality accorded him and for conversations with D. E. Aspnes, A. Baldereschi, H. Fukuyama, B. I. Halperin, J. J. Hopfield, and E. O. Kane, whose work was a basis for this paper. Help was given by Mrs. B. C. Chambers with the computer programming. At Harvard University H. Ehrenreich provided useful criticisms.

APPENDIX A: ADAPTATION OF THE HALPERIN-LAX *ANSATZ* TO THE TIGHT-BINDING MODEL

Halperin and Lax construct a variational principle for the density of states by assuming that a state centered about R_i has energy E if the potential has a relative minima at R_i, and $E = T + \sum \delta\epsilon_i p_i$. The expectation value of the kinetic energy is T and the square amplitude on a site R_i is p_i. For a high density of weak scatters we may express the constraints in terms of Lagrange multipliers and approximate certain integrals by Gaussians. The result for the density of states is:

$$\rho(E) \propto \exp\left[-\left(E - T - x\delta \sum_j p_j \right)^2 \Big/ 2x(1-x)\,\delta^2 \sum_j p_j^2 \right].$$

The expression in Sec. II follows by using as a trial function $p_i \propto e^{-aR_i}$ and minimizing the exponential with respect to a.

APPENDIX B: CALCULATION OF $\epsilon(\omega)$ IN THE CPA

For states described by the propagator in Eq. (5), the zero-wave-number dielectric constant is given by

$$\epsilon(\omega) - 1 = 4\pi e^2 \sum_{k,\sigma} \int_{-\infty}^{\infty} \frac{dx}{2\pi} f(x)\, \mathrm{Im} G(x + i\epsilon) \times \left(\frac{1}{m_{\mathrm{eff}}} \left[G^2(x+\omega+i\epsilon) + G^2(x-\omega-i\epsilon) \right] + 2\frac{k^2}{m_{\mathrm{eff}}^2} \left[G^3(x+\omega+i\epsilon) + G^3(x-\omega-i\epsilon) \right] \right).$$

The sum over wave numbers may be done exactly. We retain only the most important terms

$$\epsilon(\omega) - 1 = \frac{4\pi e^2}{m_{\mathrm{eff}}} \frac{1}{8\pi^2} (2m_{\mathrm{eff}})^{3/2} \int_{-\infty}^{\infty} f(x) \times \left[[x - \Sigma^*(x)]^{1/2} \left(\frac{1}{[\omega - \Sigma(x+\omega) + \Sigma^*(x)]^2} + \frac{1}{[\omega - \Sigma^*(x) + \Sigma^*(x-\omega)]^2} \right) \times [x - \Sigma(x)]^{1/2} \left(\frac{1}{\omega - \Sigma(x) + \Sigma^*(x-\omega)} + \frac{1}{[\omega + \Sigma(x) - \Sigma(x+\omega)]^2} \right) \right].$$

In the experiments $E_F \sim 0.3$ eV and $\omega_p \sim 0.1$ eV the real part of the self-energy is approximately a linear function in this range

$$\epsilon(\omega) - 1 \simeq \frac{4\pi n e^2}{m} \frac{1}{2} \left\{ \left[\omega \left(1 - \frac{\partial \Sigma'}{\partial E_F} \right) - 2i\Sigma'' \right]^{-2} + \left[\omega \left(1 - \frac{\partial \Sigma'}{\partial E_F} \right) \right]^{-2} \right\}.$$

The dampening near $x = 0.9$ can be as large as ω_p, making the reflectance peak somewhat difficult to locate.

---

*Supported in part by the National Science Foundation under Grant No. GH-32774.

†Junior Fellow, Society of Fellows, Harvard University.

[1] P. Soven, Phys. Rev. 156, 809 (1971).

[2] B. Velický, S. Kirkpatrick, and H. Ehrenreich, Phys. Rev. 175, 747 (1968).

[3] B. Velický, Phys. Rev. 184, 614 (1969); B. Velický and K. Levin, Phys. Rev. B 2, 938 (1970); K. Levin, B. Velický, and H. Ehrenreich, *ibid.* 2, 1771 (1970).

[4] H. Fukuyama, Prog. Theor. Phys. 42, 1284 (1969); 44, 879 (1970); H. Shiba, K. Kanada, H. Hasegawa, and H. Fukuyama, J. Phys. Soc. Jpn. 30, 972 (1971).

[5] D. Stroud and H. Ehrenreich, Phys. Rev. B 2, 3197 (1970).

[6] K. Levin and H. Ehrenreich, Phys. Rev. B 3, 4172 (1971); A. Bansil, H. Ehrenreich, L. Schwartz, and R. E. Watson, *ibid.* 9, 445 (1974).

[7] J. C. Woolley, in *Compound Semiconductors*, edited by R. K. Willardson and H. L. Goering (Reinhold, New York, 1962), p. 5.

[8] D. Weaire and M. Thorpe, Phys. Rev. B 4, 2508 (1971).

[9] E. O. Kane, in *Semiconductors and Semimetals*, edited by R. K. Willardson and A. C. Beer (Academic, New York, 1966), Vol. I, p. 75.

[10]M. L. Cohen and T. K. Bergstresser, Phys. Rev. 141, 789 (1966).
[11]J. C. Phillips, Comments Solid State Phys. 4, 9 (1971).
[12]J. C. Phillips, *Bonds and Bands in Semiconductors* (Academic, New York, 1973).
[13]J. A. Van Vechten, Solid State Commun. 11, 7 (1972).
[14](a) C. Alibert, G. Bordure, A. Langier, and J. Chevalier, Phys. Rev. B 6, 1301 (1972); (b) O. Berolo and J. C. Woolley, in *Proceedings of the Eleventh International Conference on the Physics of Semiconductors* (Polish Scientific, Warsaw, 1972), p. 1420; (c) J. S. Kline, F. H. Pollak, and M. Cardona, Helv. Phys. Acta 172, 816 (1968).
[15]J. C. Woolley and B. A. Smith, Proc. Phys. Soc. Lond. B 72, 214 (1958).
[16]J. C. Woolley, B. A. Smith, and S. G. Lees, Proc. Phys. Soc. Lond. B 69, 1339 (1956).
[17]W. M. Coderre and J. C. Woolley, Can. J. Phys. 46, 1207 (1968).
[18]M. B. Thomas and J. C. Woolley, Can. J. Phys. 49, 2052 (1971).
[19]H. Fetterman, J. Waldman, and C. M. Wolfe, Solid State Commun. 11, 375 (1972).
[20]A. G. Thompson and J. C. Woolley, Can. J. Phys. 45, 255 (1967).
[21]J. C. Woolley and J. Warner, Can. J. Phys. 42, 1879 (1964).
[22]J. D. Dow and D. Redfield, Phys. Rev. B 5, 594 (1972), and references cited therein.
[23]J. A. Van Vechten, O. Berolo, and J. C. Woolley, Phys. Rev. Lett. 29, 1400 (1972).
[24]S. S. Vishnubnaltla, B. Eyglunent, and J. C. Woolley, Can. J. Phys. 47, 1661 (1969).
[25]O. Berolo and J. C. Woolley, in Ref. 14(b), p. 1420.
[26]M. Cardona, in *Solid State Physics*, edited by H. Ehrenreich, F. Seitz, and D. Turnbull (Academic, New York, 1969), Vol. 11; M. B. Thomas and J. C. Woolley, Can. J. Phys. 49, 2052 (1971).
[27]M. J. Aubin and J. C. Woolley, Can. J. Phys. 46, 1191 (1968).
[28]E. H. van Tongerloo and J. C. Woolley, Can. J. Phys. 46, 1199 (1968).
[29]W. M. Coderre and J. C. Woolley, Can. J. Phys. 48, 463 (1970).
[30]W. M. Coderre and J. C. Woolley, Can. J. Phys. 46, 1207 (1970).
[31]M. J. Aubin, M. B. Thomas, E. H. van Tongerloo, and J. C. Woolley, Can. J. Phys. 47, 631 (1969).
[32]N. F. Mott and E. A. Davis, *Electronic Processes in Non-Crystalline Materials* (Claredon, Oxford, 1971).
[33]The Kane-formula effective mass is taken from O. Berolo, J. C. Woolley, and J. A. Van Vechten, Phys. Rev. B 8, 3794 (1973).
[34]P. Lawaetz, Phys. Rev. B 4, 3461 (1971).
[35]W. Czaja, in *Festkörperprobleme*, edited by O. Madelung (Springer, Berlin, 1971), Vol. XI, p. 65.
[36]A. Baldereschi and J. J. Hopefield, Phys. Rev. Lett. 28, 171 (1972); A. Baldereschi, (unpublished).
[37]J. Appelbaum and D. Hamann, Phys. Rev. Lett. 32, 225 (1974).
[38]J. C. Riviere, in *Solid State Surface Science*, edited by M. Green (Dekker, New York, 1969), Vol. 1.
[39]C. D. Gelatt, Jr. and H. Ehrenreich, Phys. Rev. B (to be published).
[40]J. M. Luttinger and W. Kohn, Phys. Rev. 97, 869 (1955).
[41]O. Berolo, J. C. Woolley, and J. A. Van Vechten, Phys. Rev. B 8, 3794 (1973).
[42]P. Lawaetz (unpublished).
[43]J. A. Van Vechten, Phys. Rev. 187, 1007 (1969).
[44]E. J. Johnson, in Ref. 9, Vol. 3, p. 154.
[45]P. J. Melz and I. B. Ortenburger, Phys. Rev. B 3, 3257 (1971).
[46]P. Y. Yu and M. Cardona, Phys. Rev. B 2, 3193 (1970). For some reason these authors and Ref. 11 assume the Brooks-Yu and Fan theories are mutually exclusive. Yu and Cardona cite Keffer *et al.*, who cites M. Mostoller [Ph.D. thesis (Harvard University, 1966) (unpublished)]. Both terms are present as Mostoller shows, though empirically the Debye-Waller factor accounts for most of the shift.
[47]M. L. Cohen and V. Heine, in Ref. 26, Vol. 24.
[48]In Ref. 11 Phillips estimates from the electronegativity the squared amplitudes on anion and cation sites to be $\frac{1}{2}(1 \pm f_i)$.
[49]B. I. Halperin and M. Lax, Phys. Rev. 148, 722 (1966).
[50]P. W. Anderson, Phys. Rev. 109, 1492 (1958).
[51]D. J. Thouless, in *Proceedings of the Fourth International Conference on Amorphous and Liquid Semiconductors*, edited by M. H. Cohen and G. Lucovsky (North-Holland, Amsterdam, 1972), p. 461; J. M. Ziman, J. Phys. C 1, 1532 (1968); E. N. Economou, S. Kirkpatrick, M. H. Cohen, and T. P. Eggarter, Phys. Rev. Lett. 25, 520 (1970).
[52]H. Ehrenreich, J. Phys. Chem. Solids 2, 131 (1957).
[53]T. N. Morgan, in Ref. 14(b), p. 989.
[54]A. R. Hutson, Bell Laboratories, Murray Hill, N.J. (private communication).
[55]J. D. Eshelby, in Ref. 26, Vol. 3.
[56]D. Richardson, J. Phys. C 4, L289 (1971); *ibid.* (to be published).
[57]R. Hill and D. Richardson, J. Phys. C 6, L115 (1973).
[58]P. N. Sen, Phys. Rev. B 8, 5613 (1973).
[59]A. Ebina, Y. Sato, and T. Takahashi, Phys. Rev. Lett. 32, 1366 (1974).